

Precipitation of calcium phosphate in the presence of albumin on titanium implants with four different possibly bioactive surface preparations. An in vitro study

V. Stenport · P. Kjellin · M. Andersson · F. Currie · Y.-T. Sul ·
A. Wennerberg · A. Arvidsson

Received: 26 October 2007 / Accepted: 18 June 2008 / Published online: 15 July 2008
© Springer Science+Business Media, LLC 2008

Abstract The aim of the present study was to compare the nucleating behaviour on four types of bioactive surfaces by using the simulated body fluid (SBF) model with the presence albumin. Titanium discs were blasted (B) and then prepared by alkali and heat treatment (AH), anodic oxidation (AO), fluoridation (F), or hydroxyapatite coating (HA). The discs were immersed in SBF with 4.5 mg/ml albumin for 3 days, 1, 2, 3 and 4 weeks and analysed with scanning electron microscopy/energy dispersive X-ray analysis (SEM/EDX) and X-ray photoelectron spectroscopy (XPS). Topographic surface characterisation was performed with a contact stylus profilometer. The results demonstrated that the bioactive surfaces initiated an enhanced calcium phosphate (CaP) formation and a more rapid increase of protein content was present on the bioactive surfaces compared to the blasted control surface. The observation was present on all bioactive surfaces. The fact that there was a difference between the bioactive surfaces and the blasted control surface with respect to precipitation of CaP and protein content on the surfaces support the fact that there may be biochemical advantages in vivo by using a bioactive surface.

1 Introduction

It has been suggested that a biochemical bonding between bone tissue and titanium implant surface can be obtained by using a bioactive surface modification. Bioactivity has been defined as “the characteristics of an implant material which allows it to form a bond with living tissues” [1]. Theoretically, the advantage with bioactive implants could be that the biochemical attachment is rapid, i.e. it acts at a time when no new bone has formed at the implant surface, and consequently the implants may have a more rapid fixation at an early stage. Another interpretation of the term bioactive, may be a surface material that enhance bone formation by stimulating bone forming cells resulting in a more rapid bone mineralization compared to a non bioactive material.

According to the literature, titanium treatments resulting in possibly bioactive surfaces are; (1) alkali and heat treatment (AH) [2], (2) anodic oxidation (AO) [3], (3) fluoridation (FA) [4], and (4) hydroxyapatite coatings (HA) [5]. These techniques alter both the surface chemistry and topography, and may thereby contribute to create an increased bond with the bone. However the exact mechanism of bone formation on the different surfaces is still unknown.

Various surface preparations have been evaluated in vitro by using a simulated body fluid (SBF) model. By immersion of a biomaterial in SBF, i.e. solutions with ion concentrations approximately equal to those of human blood plasma [6–8], observation of the nucleating capacity of the material can be performed. It has been suggested that the nucleation of CaP mimic the initial mineralization of bone on the implant surface. In a recent review report a correlation has been described between apatite formation in SBF models and in vivo bone bioactivities, this within the

V. Stenport (✉) · Y.-T. Sul · A. Wennerberg · A. Arvidsson
Department of Biomaterials, Göteborg University,
P.O. Box 412, 405 30 Goteborg, Sweden
e-mail: victoria.stenport@biomaterials.gu.se

V. Stenport · A. Wennerberg
Department of Prosthetic Dentistry/Dental Materials Science,
Sahlgrenska Academy, Göteborg University, P.O. Box 450,
405 30 Goteborg, Sweden

V. Stenport
Brånemarkclinic, Public Health Care, Goteborg, Sweden

P. Kjellin · M. Andersson · F. Currie
Promimic AB, Stena Center 1B, 412 92 Goteborg, Sweden

same glass–ceramic material [9]. However, compared to the SBF model the *in vivo* process is much more complex and proteins, enzymes and biological factors play an important role [10].

In a newly published study various bioactive surfaces were evaluated using a SBF model. The results indicated initial differences with increased Ca/P ratio for the fluoridated surfaces, however the difference levelled out with time [11].

Few studies have been performed by using bovine serum albumin (BSA) in various concentrations in SBF-solutions. The results from these studies indicate that the BSA alters the nucleation rate, morphology; composition and crystallinity of the CaP precipitate [10, 12, 13]. This is of interest since it has been discussed that protein adsorption may contribute to changes in cell behaviours and could thus may be regarded as a fundamentally important in the interaction between the cells and biomaterials [14]. As a consequence, it has been speculated that the protein adsorption could be related to the bioactivity of specific materials.

At present, it is still not clear if the surface material effects the CaP nucleation and how the presence of albumin alters the precipitation on various surfaces. Moreover, studies comparing CaP precipitation with BSA on surfaces claimed to be bioactive are still lacking. Therefore, the aim of the present study was to compare the nucleating behaviour of four different surfaces, suggested as bioactive, by using the SBF model with the addition of BSA.

2 Materials and methods

2.1 Surface preparations

In total 90 circular discs (\varnothing : 8 mm, thickness: 3 mm) of commercially pure titanium (grade 3) were included in the present study. The specimens were blasted with Al_2O_3 powder with a particle size of 75 μm , to increase the surface roughness. The samples were ultrasonically cleaned in diluted Extran MA01 and absolute ethanol, respectively, and dried at 60°C for 24 h. The discs were then divided into five groups, one group ($n = 18$) served as a control and was not subjected to any surface treatment prior to the SBF immersion. The other groups of samples were used for the following surface preparations.

2.1.1 Alkali and heat treatment

Alkali and heat treatment was performed as described in the literature [15–17]. The specimens ($n = 18$) were soaked in 5 M aqueous NaOH for 24 h at 60°C and were thereafter gently washed with distilled water before they

were let to dry for 24 h at 40°C. The specimens were then heated in air to 600°C by increasing the temperature by 5°C/min in an electrical furnace (Bitatherm, Beta Laboratory Furnaces, Israel), and were kept at 600°C for 1 h before being allowed to cool to room temperature in the furnace.

2.1.2 Anodic oxidation

Samples ($n = 18$) were prepared in a mixed electrolyte containing magnesium ions using the Micro Arc Oxidation (MAO) method in galvanostatic mode [3]. The electrochemical cell was composed of two platinum plates as cathodes and the titanium anode at the centre. Currents and voltages were continuously recorded at intervals of one second by an IBM computer interfaced with a DC power supply. The content of ripple was controlled to less than 0.1%. The surface properties of the oxidized group were characterized as a magnesium titanate consisting of some 9 at% Mg, 3.4 μm of oxide thickness, 24% porosity of porous structure, anatase plus rutile of crystal structure [18].

2.1.3 Fluoridation

One group of samples ($n = 18$) was fluoridated according to the technique of Ellingsen [4] the samples were immersed in an aqueous solution of 0.95 M NaF and subsequently washed twice in distilled water for 30 s. The samples were then allowed to dry at room temperature.

2.1.4 Hydroxyapatite coating

A hydroxyapatite coating was obtained by dipping the titanium discs ($n = 18$) into a stable sol which contained surfactants, water, organic solvent and crystalline nanoparticles of hydroxyapatite with a Ca/P ratio of 1.67. The diameter of the hydroxyapatite particles was approximately 10 nm. After the dipping procedure the discs were dried for half an hour in open air, allowing the organic solvent to evaporate. This was followed by a heat treatment at 550°C for 5 min under nitrogen atmosphere in order to remove all dispersing agents. The nitrogen atmosphere protected the titanium surface from further oxidation. The treatment resulted in a very thin hydroxyapatite coat on the titanium surface (less than 50 nm thick).

2.2 SBF immersion

The revised SBF (r-SBF) described by Oyane and co-workers [19] was used in the present study. It was prepared by dissolving 5.403 g NaCl (Merck, Darmstadt, Germany), 0.740 g NaHCO_3 (Merck, Darmstadt, Germany), 2.046 g Na_2CO_3 (Merck, Darmstadt, Germany), 0.225 g

KCl (Merck, Darmstadt, Germany), 0.230 g $K_2HPO_4 \cdot 3H_2O$ (Merck, Darmstadt, Germany), 0.311 g $MgCl_2 \cdot 6H_2O$ (Merck, Darmstadt, Germany), 11.928 g 2-(4-(2-hydroxyethyl)-1-piperazinyl)ethanesulfonic acid (HEPES) (Research Organics Inc., Cleveland, Ohio, USA), 0.293 g $CaCl_2$ (KEBO Lab AB, Spånga, Sweden), and 0.072 g Na_2SO_4 (Merck, Darmstadt, Germany) in 1,000 ml distilled water. HEPES was dissolved in 100 ml distilled water before being added to the solution, and the final pH was adjusted to 7.4 at 37°C. Albumin was added to result in a final concentration of 4.5 mg/ml [20].

Each specimen was immersed in 25 ml r-SBF/albumin in separate sealed polystyrene vials and kept at 37°C. Once every week the r-SBF/albumin was changed to freshly prepared solution. After immersion for 3 days, 1, 2, 3 and 4 weeks the SBF/albumin immersion was interrupted and the specimens were thoroughly rinsed with distilled water to remove any loosely attached calcium phosphate material. The specimens were then dried at room temperature and sealed in dry vials. Three samples of each type of surface were not immersed in SBF/albumin, to serve as controls for each type of surface group.

2.3 Topographical characterization

All specimens were topographically analysed after SBF immersion with a contact stylus profilometer (Surfscan 3J[®], Somicronic, France), and the specimens of each surface type that were not immersed in SBF were used as controls. The analysis was performed over a measuring area of $0.5 \times 0.5 \text{ mm}^2$, with 4 μm between scans and a stylus radius of 2 μm . Each disc was measured in one area, located in the corresponding region for all discs regardless of group.

A Gaussian filter with size $80 \times 80 \mu\text{m}^2$ was applied to separate roughness from form and waviness. Thereafter the surface roughness, in terms of the following topographical parameters, was calculated.

S_a = Arithmetic mean height deviation from a mean plane (μm).

S_{ds} = Density of summits, i.e. the number of summits of a unit sampling area (μm^{-2}).

S_{dr} = Developed interfacial area ratio, i.e. the ratio of the increment of the interfacial area of a surface over the sampling area (%).

S_{ci} = Core fluid retention index, i.e. the ratio of the void volume of the unit sampling area at the zone (5–80% bearing area) over the RMS deviation.

Mathematical descriptions of the parameters can be found in Stout et al. [21]. Calculations of group means and standard deviations for each surface preparation and time point was performed.

2.3.1 Scanning electron microscopy/energy dispersive X-ray analysis (SEM/EDX)

For the SEM analyses, a LEO Ultra 55 FEG SEM equipped with an Oxford Inca EDX system, operating at 7 kV, was used. The samples were examined without surface sputtering. Micrographs were recorded at different magnifications to investigate both the surface coverage and the morphologies of the crystals. The atomic composition was monitored using EDX analysis at two different magnifications. Analyses at a low magnification were performed on a major part of the sample to describe a mean value of the atomic composition. Analyses on individual crystals were also made in order to identify them by correlating their structure with their chemical composition. Two samples were analysed from each surface preparation and incubation time and mean value was calculated.

2.3.2 X-ray photoelectron spectroscopy (XPS)

The surface chemistry was analysed by XPS (PHI 5000 ESCA system, Perkin Elmer Wellesley, USA) with an operating angle of 45° at 300 W using a MgK excitation source. An average was calculated from two separate analyses at approximately the middle and close to the edge of two discs.

3 Results

3.1 Topographical characterization

The mean values for different surfaces and time points are presented in Table 1. In general, there were only small differences between the different surface preparations. No surface distinguished itself from the others specifically in all parameters. However, the fluoridated and anodically oxidized surfaces demonstrated increased surface area ratio (S_{dr}) after incubation for 3 days and 1 week (F) and after 3 and 4 weeks (AO).

3.1.1 S_a -mean values

The mean values calculated for each surface and time point demonstrated similar results for all surfaces except for the fluoride treated surface that was slightly rougher. The fluoridated samples demonstrated a mean value peak after 3 days of incubation and lower mean value at other time points. This pattern was not detected for the other surfaces; however the HA-surface demonstrated the highest mean value after 1 week and 3 weeks.

Table 1 Topographical results as measured with contact stylus profilometry

SBF immersion time	Surface type	<i>n</i>	S_a (μm)	S_{ds} (μm^{-2})	S_{dr} (%)	S_{ci}
0 weeks	B	3	0.56 (0.02)	1,556 (33)	1.11 (0.06)	1.61 (0.21)
	AH	3	0.56 (0.06)	1,696 (100)	1.25 (0.27)	1.61 (0.01)
	AO	3	0.54 (0.05)	1,656 (38)	1.06 (0.20)	1.54 (0.02)
	F	3	0.65 (0.04)	1,511 (37)	1.39 (0.12)	1.53 (0.05)
	HA	3	0.54 (0.05)	1,656 (38)	1.06 (0.19)	1.54 (0.02)
3 days	B	3	0.59 (0.02)	1,637 (83)	1.31 (0.15)	1.65 (0.02)
	AH	3	0.64 (0.06)	1,502 (36)	1.30 (0.08)	1.63 (0.04)
	AO	3	0.54 (0.03)	1,737 (26)	1.10 (0.20)	1.59 (0.03)
	F	3	0.98 (0.24)	1,594 (195)	4.54 (2.89)	1.76 (0.10)
	HA	3	0.54 (0.04)	1,737 (26)	1.10 (0.59)	1.59 (0.04)
1 week	B	3	0.66 (0.02)	1,741 (167)	1.97 (0.77)	1.55 (0.06)
	AH	3	0.54 (0.02)	1,408 (71)	0.98 (0.11)	1.58 (0.05)
	AO	3	0.58 (0.01)	1,654 (8)	1.29 (0.02)	1.60 (0.03)
	F	3	0.74 (0.16)	1,612 (120)	2.40 (1.16)	1.49 (0.40)
	HA	3	0.78 (0.24)	1,600 (139)	1.74 (0.59)	1.58 (0.02)
2 weeks	B	3	0.54 (0.04)	1,787 (07)	1.21 (0.24)	1.55 (0.60)
	AH	3	0.68 (0.16)	1,531 (109)	1.31 (0.38)	1.55 (0.01)
	AO	3	0.61 (0.05)	1,625 (101)	1.29 (0.02)	1.59 (0.02)
	F	3	0.63 (0.21)	1,354 (494)	1.61 (1.75)	1.60 (0.09)
	HA	3	0.66 (0.10)	1,660 (68)	1.57 (0.31)	1.61 (0.07)
3 weeks	B	3	0.57 (0.04)	1,758 (41)	1.32 (0.16)	1.59 (0.04)
	AH	3	0.60 (0.04)	1,512 (27)	1.23 (0.05)	1.65 (0.01)
	AO	3	0.68 (0.14)	16,791 (101)	2.82 (2.59)	1.48 (0.24)
	F	3	0.63 (0.17)	1,687 (127)	1.73 (1.18)	1.61 (0.05)
	HA	3	0.82 (0.33)	1,573 (171)	1.55 (0.17)	1.56 (0.11)
4 weeks	B	3	0.69 (0.04)	1,745 (66)	1.68 (0.35)	1.58 (0.01)
	AH	3	0.62 (0.01)	14,752 (41)	1.33 (0.05)	1.63 (0.01)
	AO	3	0.77 (0.16)	1,831 (115)	4.24 (3.66)	1.41 (0.31)
	F	3	0.67 (0.12)	1,685 (158)	1.89 (1.21)	1.61 (0.01)
	HA	3	0.71 (0.16)	1,695 (145)	1.49 (0.23)	1.60 (0.10)

B: blasted titanium, AH: alkali and heat treated, AO: anodically oxidized, F: fluoridated, and HA: hydroxyapatite coated. The figures represent means, standard deviations within parenthesis

3.1.2 S_{ds} -mean values

In general, all samples demonstrated denser surfaces with increasing incubation time. On the blasted samples the surface density was initially increased and but not after 2nd week. The density of the AO, HA, and F group increased initially, however decreased after 3 days (AH) or 1 week (AO, HA) and increased again after 2 weeks. The F samples demonstrated an increased density until the 1st week, and decreased after 2 weeks.

3.1.3 S_{dr} -mean values

The F group demonstrated a highly increased surface area after 3 days, which decreased until 2nd week and increased again thereafter but not to the same level. For the HA and B groups, the surface area increased until 1st week followed by a decrease after the 2nd week. The AO group showed a

gradually increased surface area with a high peak at 4 weeks.

3.1.4 S_{ci} -mean values

The mean values of this parameter demonstrated small variations at all time point for all groups. The F group increased more after 3 days but was at the same level as the other groups thereafter. The AO group's mean values were at the same level as for the other group initially, however after the 2nd week the mean values gradually decreased.

3.2 SEM/EDX

3.2.1 Blasted samples

The blasted samples had small amounts of crystals on the surfaces after 3 days and 1 week. At 3 weeks the amount

of crystals were markedly increased. Dark carbonate containing areas was observed and increased rapidly after 4 weeks (see Fig. 1).

3.2.2 Alkali-heat treated samples

After 3 days a small amount of crystals were observed on the surfaces. After 2 weeks calcium and phosphate containing rice-shaped crystals were present on the surface, which increased after 3 and 4 weeks. Several dark carbonate containing areas were present at 3 days and the areas without the carbonate appeared to have a high porosity. SEM pictures from 3 days and 4 weeks are presented in Fig. 2.

3.2.3 Anodically oxidized samples

After 3 days and 1 week there were a few crystals on the surface together with small dark areas of carbonate containing material. After 2 weeks the CaP containing rice-shaped crystals had formed on the surface and after 3–4 weeks these crystals existed in larger amounts. The dark areas containing carbonate appeared to gradually increase until the 4th weeks, when the dark layer was thick and partly covered the porous surfaces. SEM picture from 3 days and 4 weeks are presented in Fig. 3.

3.2.4 Hydroxyapatite samples

The HA samples had few crystals on the surface with a high percentage of carbonate. At 3 weeks small rice-like crystals with a high calcium and phosphate content began to form. The number of crystals increased after 4 weeks, however the surfaces were still incompletely covered after 4 weeks. SEM picture from 3 days and 4 weeks are presented in Fig. 4.

3.2.5 Fluoridated samples

A few crystals were visible from 3 days and the amount increased with time. After 1 and 2 weeks many areas with dark carbonate containing material were visible. After 4 weeks the fluoridated surface showed crack formation and appeared to dissolve. SEM pictures after 3 days and 4 weeks are presented in Fig. 5.

3.3 EDX

The atom percentages from EDX measurements of each surface preparation and time point are presented in Table 2.

In general, percentages of titanium were observed to decrease with increased immersion time for all surfaces.

Fig. 1 SEM pictures of a blasted sample, after 3 days and 4 weeks

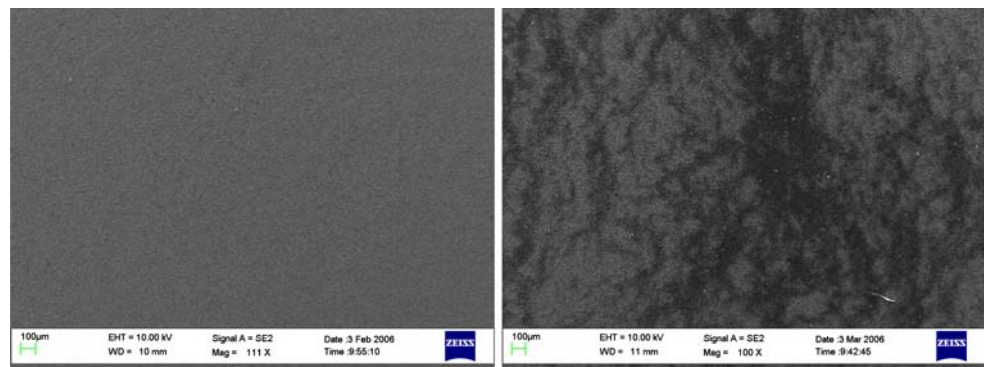


Fig. 2 SEM picture from an alkali-heat treated sample, after 3 days and 4 weeks

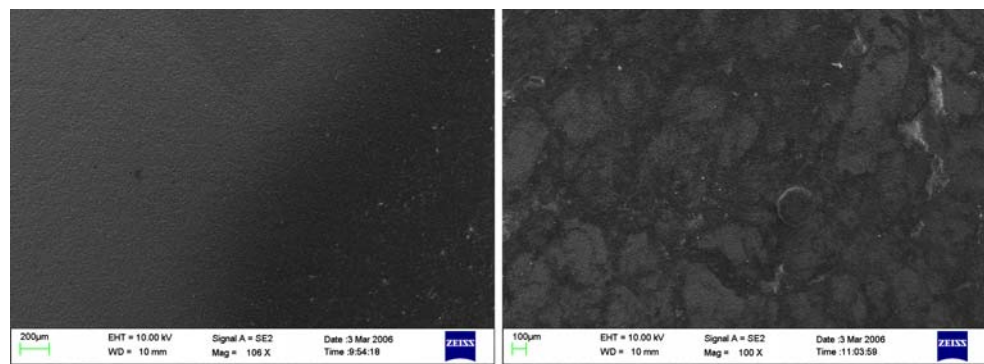


Fig. 3 SEM picture from an anodically oxidized sample, after 3 days and 4 weeks

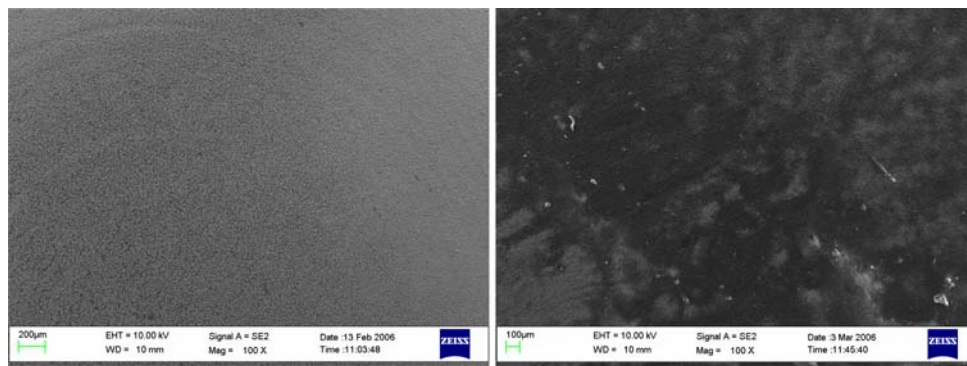


Fig. 4 SEM picture from a hydroxyapatite coated sample, after 3 days and 4 weeks

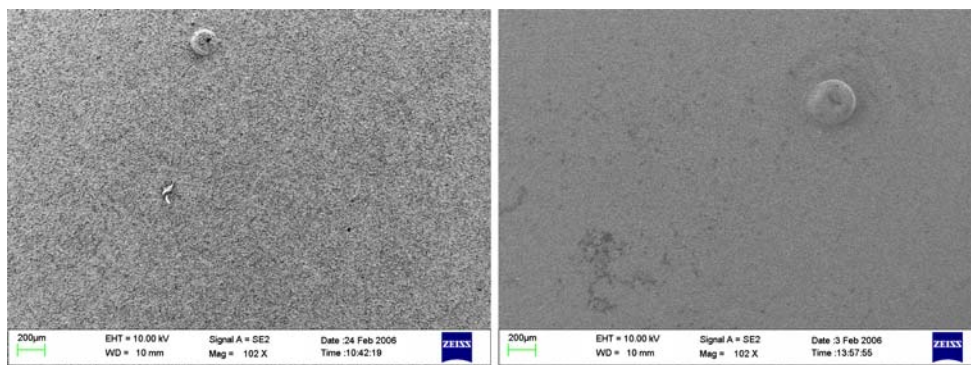
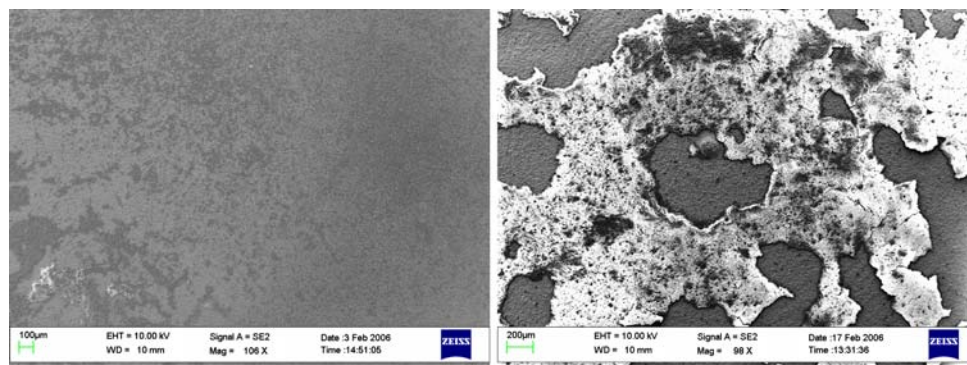


Fig. 5 SEM picture from a fluoridated sample, after 3 days and 4 weeks



The bioactive surfaces i.e. the F, AH, AO and HA treated samples demonstrated calcium and phosphate signals at an earlier stage compared to the blasted control samples. The AO surface showed calcium on the surface after 2 weeks, however F, AH and HA samples had calcium on the surface after 3 days.

3.4 XPS

In general, the samples demonstrated decreased levels of titanium (Ti) after 3 days of incubation compared to the control samples. The F and AH treated samples showed decreased Ti levels after 1 week, however after 4 weeks all samples had low levels of Ti on surfaces (for details see Fig. 6).

The levels of nitrogen (N) (with a binding energy of 398 eV) were increased on all samples after 3 days

compared to baseline levels, however the blasted control samples had half the amount of N on the surfaces compared to the bioactive surfaces after 3 days. The bioactive surfaces reached their peak level after 3 days in contrast to the blasted sample that reached a maximum after 2 weeks. The AO surface had stable level of for N for all time point after 3 days, compared to the other surfaces that demonstrated some fluctuations of the amount of nitrogen at different time points (for details see Fig. 7).

The most rapid increase in Ca/P formation was observed on the AO samples followed by the F samples. The HA samples that were coated with a layer of nano HA showed decreased levels of Ca/P initially. The AH and HA treated samples had increased Ca/P values after 1 week of incubation. The B samples (controls) started to show increased Ca/P value after the 2nd week. After 4 weeks of incubation

Table 2 Mean value of atom% of titanium (-Ti), calcium (-Ca) and phosphates (-P) on the surfaces examined by EDX after incubation for 3 days, 1, 2, 3 and 4 weeks

	Ctr	3 days	1 week	2 weeks	3 weeks	4 weeks
Ti						
B-Ti	27.3(0.9)	24.0(0.2)	24.5(1.3)	25.8(1.5)	21.2(2.8)	14.3(5.2)
AH-Ti	17.7(0.5)	12.6(3.5)	15.2(0.2)	15.3(2.9)	15.8(0.3)	9.2(5.3)
AO-Ti	20.9(0.5)	18.2(2.5)	22.3(21.8)	16.1(5.4)	10.5(0.2)	2.6(0.4)
F-Ti	25.3(13.9)	30.9(17.2)	15.6(17.2)	38.8(20.6)	12.8(0.1)	16.8(1.9)
HA-Ti	20.8(3.8)	33.3 (1.9)	19.8(6.7)	24.4(0.2)	25.5(2.2)	22.0(2.5)
Ca						
B-Ca	0	0	0	0	0	0.5(0.5)
AH-Ca	0	2.4(0.9)	3.9(0.4)	4.0(0.3)	4.3(0.9)	2.9(0.6)
AO-Ca	0	0	0	0.4(0.4)	1.1(0.6)	0.8(0.1)
F-Ca	0	0.3(0.3)	1.9(1.9)	1.2(1.2)	1.3(0.2)	2.3(0.7)
HA-Ca	2.1(1.7)	0.4(0.1)	3.9(3.2)	0.3(0.3)	0.7(0.3)	0.8(0.5)
P						
B-P	0	0	0	0	0	0.5(0.5)
AH-P	0	0	0.7(0.3)	1.3(0.6)	1.4(0.8)	1.1(0.2)
AO-P	1.3(0.1)	1.3(0.2)	1.2(0.2)	1.8(0.2)	1.7(0.1)	1.8(0.4)
F-P	0	0.3(0.3)	1.0(1.0)	0.8(0.8)	1.9(0.2)	1.9(0.1)
HA-P	2.1(1.8)	0.4(0.1)	3.48(2.9)	0.4(0)	0.7(0.3)	0.8(0.1)

Standard deviations within parenthesis. B: blasted titanium, AH: alkali and heat treated, AO: anodically oxidized, F: fluoridated and HA: hydroxyapatite coated

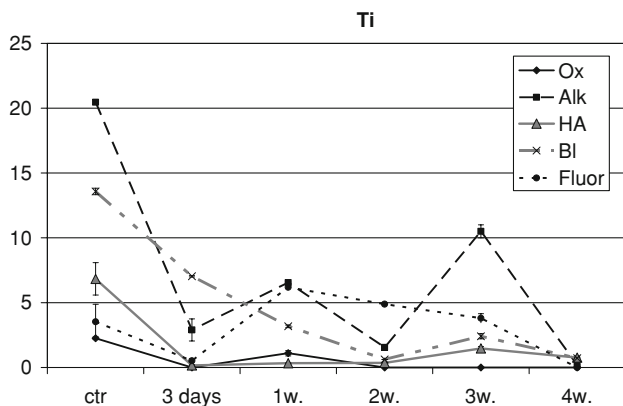


Fig. 6 Atom% of titanium as measured with XPS. Mean values and vertical bars for standard deviations are presented B: blasted titanium, AH: alkali and heat treated, AO: anodically oxidized, F: fluoridated and HA: hydroxyapatite coated

in SBF the alkali-heat treated samples demonstrated the highest value of all the surfaces tested (for details see Fig. 8).

4 Discussion

The results of the present study demonstrated a more rapid calcium formation and nitrogen presence on the bioactive surfaces compared to the blasted control. However the

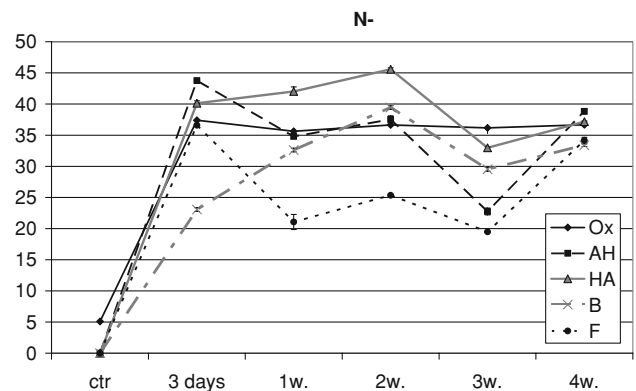


Fig. 7 Atom% of nitrogen (N-) as measured with XPS. Mean values and vertical bars for standard deviations are presented. B: blasted titanium, AH: alkali and heat treated, AO: anodically oxidized, F: fluoridated, and HA: hydroxyapatite coated

effect levelled out after 4 weeks. This was observed on all bioactive surfaces, however the Ca/P ratio of the anodically oxidized and fluoridated surfaces increased after 3 days compared to the alkali-heat treated and HA coated surfaces that increased after 1 week. In the present study the N-levels were evaluated and interpreted as an indication of albumin presence on the titanium surfaces. The nitrogen content of the amide groups of the protein has previously been used as an indirect way to show the presence of proteins [14].

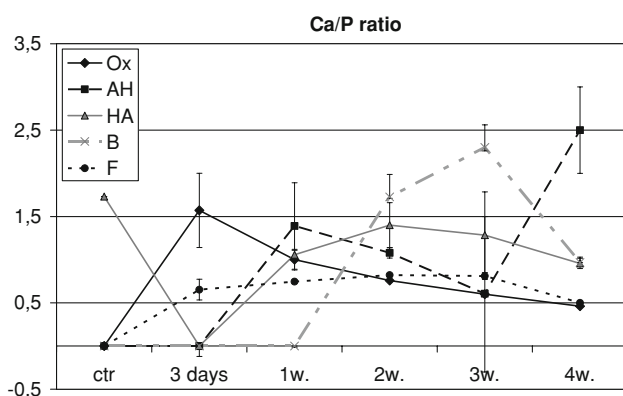


Fig. 8 Calcium/phosphate ratio calculated from XPS measurements. Mean values and vertical bars for standard deviations are presented. B: blasted titanium, AH: alkali and heat treated, AO: anodically oxidized, F: fluoridated, and HA: hydroxyapatite coated

The topographical surface roughness evaluations demonstrated that the surfaces were minimally rough [20] and that the roughness parameters (S_a , S_{ds} , S_{dr}) increased with increased incubation time, thus indicating a rougher surface due to the CaP adherence on the surfaces.

In the present study a revised SBF (rSBF) solution [19] was used. This solution has ion concentrations similar to human blood plasma [22]. It has been observed that the rSBF has a strong tendency of spontaneous precipitation; however due to the fact that the ion concentration is close to human blood plasma this SBF version was chosen in the present study. It has been discussed whether a static or dynamic SBF model is the most accurate to use [23]. The previously mentioned study has also demonstrated that a static model may favour the precipitation as well as a rougher surface. However in the present study, the buffer was changed once a week to remove precipitated material from the buffer. Moreover, the samples were thoroughly rinsed after incubation to eliminate loose particles from the samples. Furthermore, the topography of the used surfaces had baseline mean values with small differences, minimizing differences due to passive attachment of unbound precipitate due to differences in roughness. Since all surface preparations were tested in a similar experimental model the effect from a possible spontaneous precipitation were the same for all surface preparations.

Several studies have reported that the presence of albumin decreased the amount of CaP precipitate on a surface [13]. The result from the present study can support such a statement. The results were comparable to the results from a similar study with the same surface preparations, where increased amounts of CaP was reported after 4 weeks in an SBF study without albumin [11]. In the present study an albumin concentration close to human blood plasma was used, however several studies have used a lower concentration [24–26]. Albeit a lower concentration, the results in

the literature indicate that lower concentrations inhibit the CaP precipitation, by the absorption of protein into the amorphous calcium and phosphate layer [24]. In a study by Combes et al. [13] it was observed that the CaP precipitation decreased by 65% at an albumin concentration close to human blood plasma (5 mg/ml).

In the present study a pH of 7.4 was used. This pH was chosen since this is close to the physiologic pH of blood plasma. However, in conjunction to a trauma, as the implant insertion in bone, the pH is lowered and hence the protein adsorption may be altered. The fact that a change to a lower pH affects the absorption of albumin has been described by Wasell et al. In that study it was observed that BSA was more strongly adsorbed under acidic conditions onto titanium powder [27].

The fact that there was a difference between the suggested bioactive surfaces and the blasted control surface, with respect to precipitation of CaP and albumin amount on the test surfaces, supports the fact that there may exist biochemical advantages in vivo by using a bioactive surface. However the bone formation process on titanium surfaces needs further investigation to discriminate between various bioactive surfaces and actions of other proteins and their interactions.

Acknowledgements The authors thank Christian Erneklint at the Dept of Prosthetic Dentistry/Dental Materials Science, Göteborg University for kindly heat treating the alkali specimens. The authors also thank the Swedish Research Council, Hjalmar Svensson Research Foundation, Knut and Alice Wallenberg Foundation, the Wilhelm and Martina Lundgren Science Foundation, the Royal Society of Arts and Sciences in Göteborg, the Adlerbert Foundation, the Biointerface project of the Ministry of Science and Technology, Republic of Korea for financial support.

References

1. L. Hench, *Handbook of bioactive ceramics* (CRC press, Boca Raton, 1990), p. 7
2. H.M. Kim, F. Miyaji, T. Kokubo, T. Nakamura, *J. Mater. Sci. Mater. Med.* **8**, 341 (1997). doi:10.1023/A:1018524731409
3. Y.T. Sul, C. Johansson, E. Byon, T. Albrektsson, *Biomaterials* **26**, 6720 (2005). doi:10.1016/j.biomaterials.2005.04.058
4. J.E. Ellingsen, *J Mater Sci Mater Med* **6**, 749 (1995). doi: 10.1007/BF00134312
5. M. Gottlander, T. Albrektsson, L.V. Carlsson, *Int. J. Oral Maxillofac. Implants* **7**, 485 (1992)
6. T. Kokubo, H. Kushitani, S. Sakka, T. Kitsugi, T. Yamamuro, *J. Biomed. Mater. Res.* **24**, 721 (1990). doi:10.1002/jbm.820240607
7. T. Peltola, M. Patsi, H. Rahiala, I. Kangasniemi, A. Yli-Urpo, *J. Biomed. Mater. Res.* **41**, 504 (1998). doi:10.1002/(SICI)1097-4636(19980905)41:3<504::AID-JBM22>3.0.CO;2-G
8. H. Takadama, H.M. Kim, T. Kokubo, T. Nakamura, *J. Biomed. Mater. Res.* **57**, 441 (2001). doi:10.1002/1097-4636(20011205)57:3<441::AID-JBM1187>3.0.CO;2-B
9. T. Kokubo, H. Takadama, *Biomaterials* **27**, 2907 (2006). doi: 10.1016/j.biomaterials.2006.01.017

10. Y. Liu, P. Layrolle, J. De Bruijn, C. Van Blitterswijk, K. De Groot, J. Biomed. Mater. Res. **57**, 327 (2001). doi:10.1002/1097-4636(20011205)57:3<327::AID-JBM1175>3.0.CO;2-J
11. A. Arvidsson, V. Franke Stenport, M. Andersson, P. Kjellin, T. Sul, A. Wennerberg. J. Mater. Sci. **18**, 1945 (2007)
12. H. Wen, J. de Wijn, K. De Groot, J. Biomed. Mater. Res. **46**, 245 (1999). doi:10.1002/(SICI)1097-4636(199908)46:2<245::AID-JBM14>3.0.CO;2-A
13. C. Combes, C. Rey, M. Freche, J. Mater. Sci. **10**, 153 (1999). doi: [10.1023/A:1008933406806](https://doi.org/10.1023/A:1008933406806)
14. H. Zeng, K. Chittur, W. Laceyfield, Biomaterials **20**, 377 (1999). doi:[10.1016/S0142-9612\(98\)00184-7](https://doi.org/10.1016/S0142-9612(98)00184-7)
15. H. Takadama, H.M. Kim, T. Kokubo, T. Nakamura, J. Biomed. Mater. Res. **57**, 441 (2001). doi:10.1002/1097-4636(20011205)57:3<441::AID-JBM1187>3.0.CO;2-B
16. H.M. Kim, F. Miyaji, T. Kokubo, T. Nakamura, J Mater Sci Mater Med **8**, 341 (1997). doi:[10.1023/A:1018524731409](https://doi.org/10.1023/A:1018524731409)
17. H.M. Kim, F. Miyaji, T. Kokubo, S. Nishiguchi, T. Nakamura, J. Biomed. Mater. Res. **45**, 100 (1999). doi:10.1002/(SICI)1097-4636(199905)45:2<100::AID-JBM4>3.0.CO;2-0
18. Y.T. Sul, C.B. Johansson, Y. Jeong, T. Albrektsson, Med. Eng. Phys. **23**, 329 (2001). doi:[10.1016/S1350-4533\(01\)00050-9](https://doi.org/10.1016/S1350-4533(01)00050-9)
19. A. Oyane, H.M. Kim, T. Furuya, T. Kokubo, T. Miyazaki, T. Nakamura, J. Biomed. Mater. Res. **65A**, 188 (2003). doi:[10.1002/jbm.a.10482](https://doi.org/10.1002/jbm.a.10482)
20. T. Albrektsson, A. Wennerberg, Int. J. Prosth. **17**, 536 (2004)
21. K.J. Stout, P.J. Sullivan, W.P. Dong, E. Mainsah, N. Luo, T. Mathia et al., *The development of methods for characterisation of roughness in three dimensions. EUR 15178 EN of commission of the European Communities* (University of Birmingham, Birmingham, 1993)
22. A.J. Vander, J.H. Sherman, D.S. Luciano, in *Human physiology. The mechanisms of body function*, 5th ed. (McGraw-Hill Publishing Company, New York, 1990), p. 349
23. X. Lu, Y. Leng, X. Zhang, J. Xu, L. Qin, C. Chan, Biomaterials **26**, 1793 (2005). doi:[10.1016/j.biomaterials.2004.06.009](https://doi.org/10.1016/j.biomaterials.2004.06.009)
24. S. Areva, H. Pladan, T. Peltola, T. Närhi M. Jokinen, M. Lindèn, Biomed. Mater. Res. **70A**:169 (2004). doi:[10.1002/jbm.a.20120](https://doi.org/10.1002/jbm.a.20120)
25. Y. Liu, E. Hunziker, P. Layrolle, C. Van Blitterwijk, P. Calvert, K. De Groot, J. Biomed. Mater. Res. **67A**, 1155 (2003). doi: [10.1002/jbm.a.20019](https://doi.org/10.1002/jbm.a.20019)
26. Y. Liu, E. Hunziker, N. Randall, K. De Groot, P. Layrolle, Biomaterials **24**, 65 (2003). doi:[10.1016/S0142-9612\(02\)00252-1](https://doi.org/10.1016/S0142-9612(02)00252-1)
27. D. Wasell, G. Embery, Biomaterials **17**, 859 (1996). doi: [10.1016/0142-9612\(96\)83280-7](https://doi.org/10.1016/0142-9612(96)83280-7)